095031
(4)

Internal architecture, permeability structure, and hydrologic significance of contrasting fault-zone types

Geoffrey C. Rawling
Laurel B. Goodwin
John L. Wilson
Department of Earth and Environmental Science, New Mexico Tech, Socorro, New Mexico 87801, US

RECEIVED
MAR 12 2007
BY

ABSTRACT

The Sand Hill fault is a steeply dipping, large-displacement normal fault that cuts poorly lithified Tertiary sediments of the Albuquerque basin, New Mexico, United States. The fault zone does not contain macroscopic fractures; the basic structural element is the deformation band. The fault core is composed of foliated clay flanked by structurally and lithologically heterogeneous mixed zones, in turn flanked by damage zones. Structures present within these fault-zone architectural elements are different from those in brittle faults formed in lithified sedimentary and crystalline rocks that do contain fractures. These differences are reflected in the permeability structure of the Sand Hill fault. Equivalent permeability calculations indicate that large-displacement faults in poorly lithified sediments have little potential to act as vertical-flow conduits and have a much greater effect on horizontal flow than faults with fractures.

Keywords: fault zone, fractures, groundwater movement, permeability, numerical models.

INTRODUCTION

Brittle fault zones in the upper crust exert significant control on subsurface fluid flow. Flow regimes in faulted sedimentary basins are strongly affected by differences in permeability of fault zones relative to their host rocks (Bredehoeft et al., 1992; Haneberg, 1995). Studies in hydrocarbon reservoirs have shown that individual fault zones may seal in some areas and leak in others, as a complex function of host-rock lithology, the deformation mechanisms operative during faulting, and fault zone diagenesis (e.g., Smith, 1980; Yielding et al., 1997). Fault zones are heterogeneous structures that cannot be simply defined as either barriers or conduits for fluid flow in either space or time (Knipe, 1993; Caine et al., 1996).

Consensus has grown among many workers on a simple and widely applicable structural and hydrologic model for faults formed in crystalline and lithified sedimentary rocks (e.g., Chester et al., 1993; Caine et al., 1996; hereafter abbreviated fault with fractures [FWF]; cf. Goodwin et al., 1999). The basic structural component is the fracture (a surface across which the rock has broken and lost cohesion), and the model is composed of three architectural elements: (1) the protolith, which is unfaulted, but may contain regional structures; (2) the damage zone, which may contain small faults, fractures, fracture networks, and veins; and (3) the core zone, which is composed of breccia and/or cataclasite, or gouge, in varying states of induration. The core zone is flanked by the damage zone and is the locus of most of the displacement. Various combinations and degrees of development of damage and core zone yield a range of possible fault-zone architectures and permeability structures (Caine et al., 1996).

The growing need for accurate simulation of subsurface fluid-flow regimes requires incorporating at least the bulk hydrologic properties of fault zones into numerical flow models. Many heavily developed aquifers in urban areas in the southwestern United States are in poorly lithified Tertiary sediments that are pervasively cut by normal faults (Mifflin, 1988; Thorn et al., 1993). In this paper, we contrast the current model of fault-zone architecture and permeability structure, developed for FWFs, with a new model for large-displacement faults in poorly lithified sediments. Our model is based on the Sand Hill fault zone in the Albuquerque basin, New Mexico. The results indicate that large-displacement faults in poorly lithified sediments have less potential to act as vertical-flow conduits and are significant impediments to cross-fault flow over a wider range of scales than FWFs. This difference is in part due to the absence of macroscopic fractures associated with faulted poorly lithified sediments.

SAND HILL FAULT

The Sand Hill fault, one of the major normal faults bounding the Rio Grande rift, marks the western margin of the Albuquerque basin (Hawley et al., 1995; Fig. 1). It is a growth fault juxtaposing synrift sediments of the Pliocene-Pleistocene upper Santa Fe Group against middle Miocene to Oligocene sediments of the lower and middle Santa Fe Group, with displacement increasing from ~10 to ~600 m downdip (Hawley et al., 1995; Heynekamp et al., 1999). The lower Santa Fe Group sediments are dominantly fine-grained sand, with subordinate medium-grained sand, silty sand, and mud. The upper Santa Fe Group sediments include sand, silt, and mud, locally capped by gravel (Heynekamp et al., 1999). Excepting zones of calcite cementation (Mozley and Goodwin, 1995), all of the materials in the fault zone are friable and easily disaggregated.

Faults in poorly lithified sediments have deformation bands (narrow, tabular zones of displacement, compaction, and/or cataclasis; cf. Aydin and Johnson, 1978) as the basic structural element and do not contain macroscopic fractures (Heynekamp et al., 1999; Sigda et al., 1999; Fig. 2). However, large-displacement "deformation band faults" in poorly lithified sediments (hereafter abbreviated DBF), exemplified by the Sand Hill fault, have two significant differences from faults described previously in high-porosity sandstones (e.g., Aydin and Johnson, 1978; Underhill and Woodcock, 1987; Antonellini and Aydin, 1995): (1) Where displacement is greater than the local mean bed thickness, a new fault-zone architectural element—the mixed zone—develops between the damage zone and the fault core (Mozley and Goodwin, 1995; Heynekamp et al., 1999; Sigda et al., 1999; Fig. 2). The mixed zone includes rotated and attenuated beds and areas where disparate sediment types are mixed at the grain scale by particulate flow during slip. Its grain-size distribution ranges from clay to sand to gravel to virtually any tectonic combination thereof. It is easily identified in the field and is lithologically, structurally, and hydrologically (Fig. 3) distinct from the core and damage zones. Where coarse grained, the basinward hanging-wall mixed zone of the Sand Hill fault is typically cemented with calcite. (2) The fault core is a foliated clay layer as thick as 10 cm. Gaps in the clay core are rare, even where the host sediments are dominantly sand (Heynekamp et al., 1999). In contrast, at displacements of >1 m, DBFs in lithified, high-porosity sandstones have a "core" that is a discrete, slickenside slip surface (Antonellini and Aydin, 1995).

METHODS

We measured the permeability of poorly lithified sandy to moderately clay-rich (up to

© 2001 Geological Society of America. For permission to copy, contact Copyright Clearance Center at www.copyright.com or (978) 750-8400.

14671

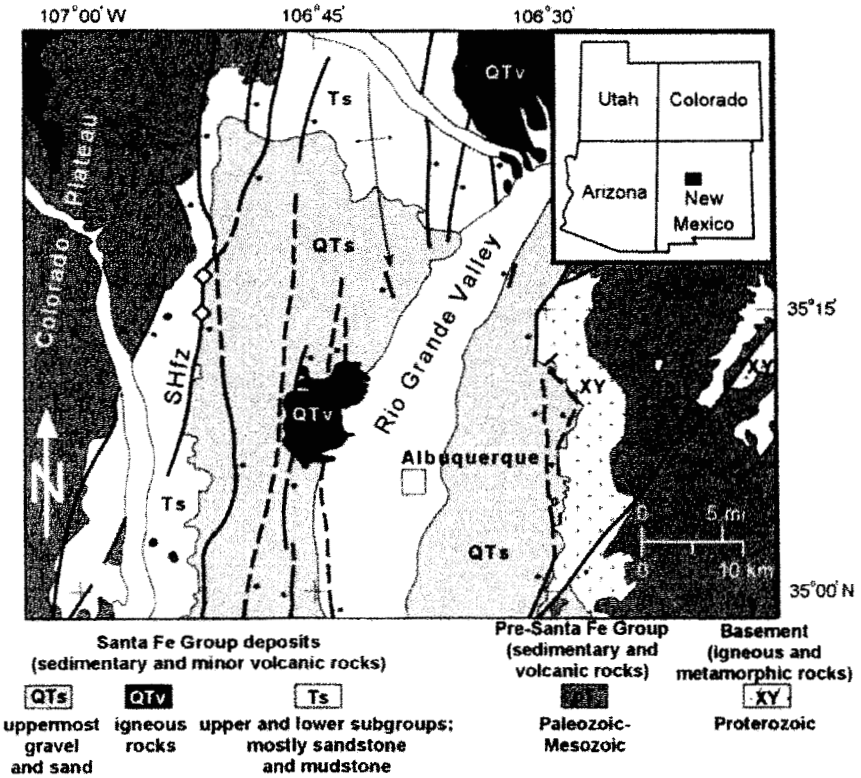

Figure 1. Study sites (open diamonds) along Sand Hill fault zone (SHfz) in Albuquerque basin of Rio Grande rift. Inset shows location. Faults are generalized; not all faults are shown. Modified from Hawley et al. (1995) and Hawley (1996).

Figure 2. Shear zone of coalesced deformation bands (dbsz, outlined by dashed lines) forming contact between footwall damage zone (fdz) and footwall mixed zone (fmz) within Sand Hill fault zone. Offset is at least several meters. Solid lines delineate tilted bedding in footwall damage zone and clay-rich (c), white sand (ws), and red sand (rs) beds transposed into foliation in footwall mixed zone. Width of area shown is 3 m.

13 wt%) sediments from the damage and mixed zones on three strike-perpendicular outcrops of the Sand Hill fault with a portable air mini-permeameter designed and built at the University of New Hampshire by M. Davis. The permeability of cemented mixed-zone sand was measured with the same device on cut surfaces of ~0.25 m^3 samples. The permeability of clay and sandy or silty clay from the footwall mixed zone and fault core was measured in consolidation tests performed on undisturbed water-saturated samples collected with coring tubes from outcrop excavations (cf. Das, 1983). The tests were performed both parallel and perpendicular to bedding and foliation. Values reported are for consolidation pressures of 10 to 18 MPa. These data are presented in Figure 3 (see also Data Repository[1]) and compared with permeability data from the literature for FWFs in crystalline rocks at effective stress conditions of 10 MPa or less.

[1]GSA Data Repository item 200110, Appendix 1. Raw permeability data, is available on request from Documents Secretary, GSA, P.O. Box 9140, Boulder, CO 80310-9140, editing@geosociety.org, or at www.geosociety.org/pubs/ft2001.htm.

DISCUSSION

Permeability Data

The bulk permeability structure of a fault zone is a consequence of the hydrologic properties of the architectural elements, their spatial arrangement, and their setting in the flow system (e.g., Caine and Forster, 1999). Both air mini-permeameter measurements and laboratory tests have sample volumes on the scale of cubic centimeters; as such, both data sets are an incomplete characterization of the macroscale hydrologic properties of the respective architectural elements. As noted by Evans et al. (1997), the data for an FWF damage zone are a lower bound on the bulk permeability of this architectural element, because the samples do not include the macroscopic fracture networks found in FWFs, which may greatly enhance permeability. Similar scaling considerations apply to DBFs but are less important because of the lack of fractures.

The hydrologic distinction between FWFs in lithified rocks and DBFs in poorly lithified sediments is clear. Fracture networks enhance permeability in the damage zone of FWFs relative to the protolith and core. The data from the Sand Hill fault indicate that in a poorly lithified DBF, deformational and diagenetic processes and the absence of fractures all reduce permeability in the damage zone, mixed zone, and core relative to a sand-rich protolith, and at best yield a small increase in permeability in the mixed zone relative to a clay-rich protolith (Fig. 3).

Bulk Hydrologic Properties

We examine the horizontal and vertical equivalent permeability ratio ($k_{faulted}/k_{unfaulted}$) of a two-dimensional cross-sectional groundwater-flow model grid block containing a fault. Two simple, idealized, end-member fault-protolith systems are considered: an FWF in crystalline rock and a DBF with mixed zones in a two-layer (sand and clay) unlithified sedimentary protolith (Fig. 4). For both models, each architectural element is assumed to be internally isotropic and homogeneous, and its permeability is assigned from the data in Figure 3. The damage zone, fault-zone thickness variations, mixed zone heterogeneity, and juxtaposition of different hanging-wall and footwall lithologies are not considered in the unlithified DBF model. The FWF system is treated as a vertically layered medium, in which equivalent permeabilities for horizontal and vertical flow regimes are weighted harmonic and arithmetic means, respectively. Equivalent permeabilities for the faulted poorly lithified sedimentary system are taken as the geometric means of the Cardwell and Parsons upper and lower bounds for flow in the horizontal and vertical directions (Renard and de Marsily, 1997, p. 257). These bounds are the most general (Renard and de Marsily, 1997, p. 271), and given the geologic simplifications and ranges in the permeability

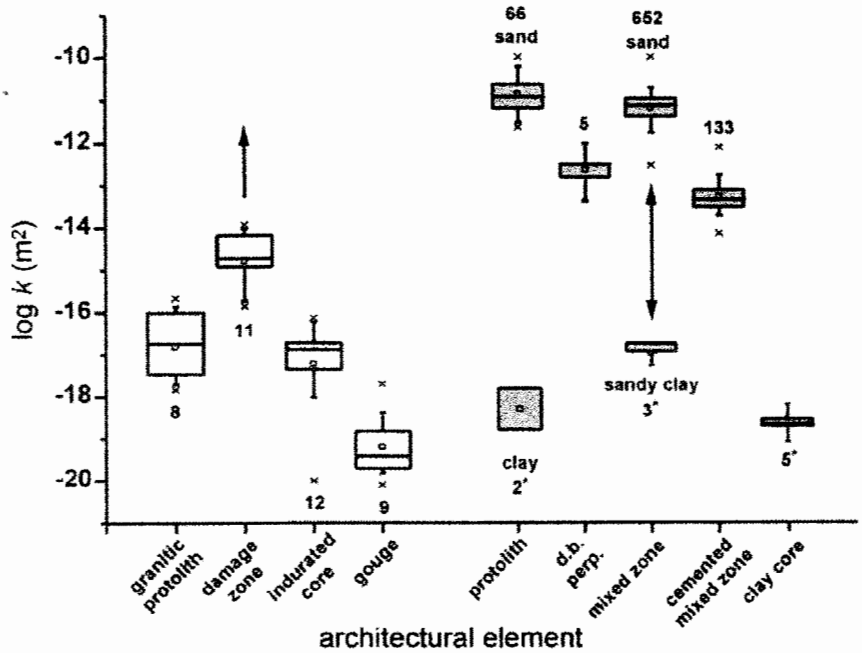

Figure 3. Permeability data for FWFs in crystalline rocks (open boxes) and DBF (gray boxes). Boxes encompass 50% of data; whiskers and x's show extrema; intermediate line is median; small open squares indicate means. Granitic protolith, damage zone, and core data are from Evans et al. (1997); gouge data are from Morrow et al. (1981, 1984). Single-headed arrow indicates that FWF damage zone data are minimum values. Measurements perpendicular to plane of deformation bands (d.b. perp.) from Sigda et al. (1999). Number of measurements is indicated next to each box; stars indicate consolidometer test data; other DBF data are air mini-permeameter measurements. Double-headed arrow indicates that mixed zone permeability varies between end members.

data, a more elaborate treatment is not justified.

The permeability trends of Figure 3 are reflected in the differences in the equivalent permeabilities of the two model grid blocks (Fig. 4). For typical grid blocks in regional groundwater-flow models, the relative fault-zone thickness, expressed as log (F_t), ranges from about −1.5 to −3 for a 10-m-wide fault zone. In this range, the horizontal equivalent permeability of the unlithified DBF system relative to the two-layer undeformed protolith system is reduced as much as four orders of magnitude, and there is little increase in vertical equivalent permeability (Fig. 4). The negligible effect of sand content (T_s) and the large effect of a small percentage of fault in the block (e.g., at log (F_t) = −4) indicate that even a very thin fault with a clay core controls the equivalent permeability of this system. Increased complexity in the model either has minimal effect or will amplify the results (e.g., inclusion of the damage zone or juxtaposition of clay mixed zone against sand protolith). Conversely, over the same range of log (F_t) values, the FWF system exhibits enhanced vertical permeability and negligible reduction in horizontal permeability at the regional scale.

Several lines of evidence suggest that at shallow (<2 km) depths in extensional systems, increasing effective stress will lower absolute permeability but will not change the relative permeabilities of the architectural el-

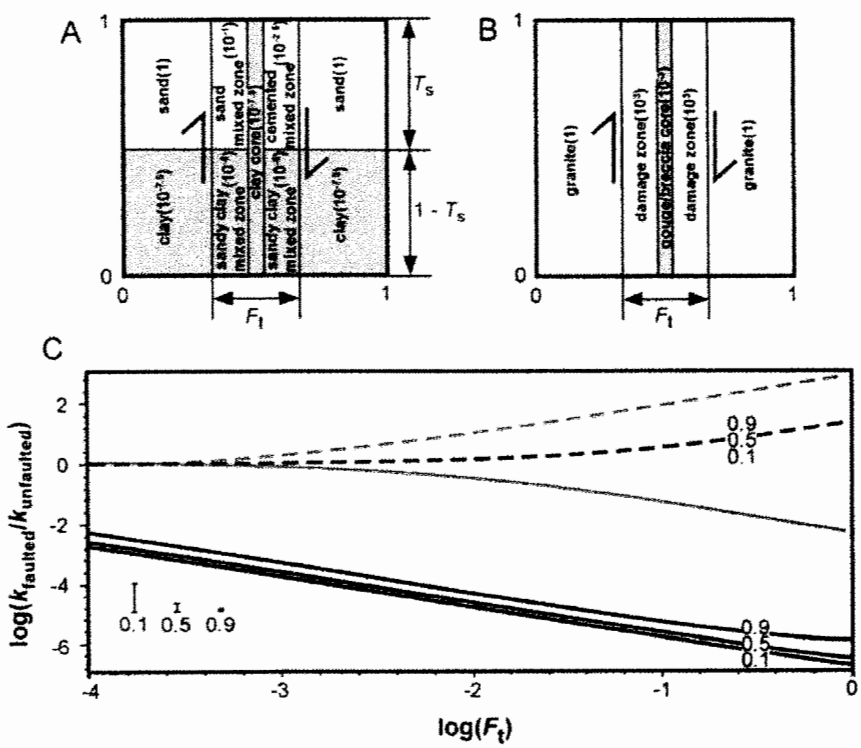

Figure 4. Hydrologic models and results of equivalent permeability calculations. A: Schematic illustration of DBF in poorly lithified sediment. Permeabilities (in parentheses) normalized to sand protolith. B: Model of FWF in crystalline rock. Permeabilities normalized to granite protolith. In both models, F_t is relative fault-zone width, as a fraction of the horizontal domain width; core width is fixed at F_t/5. T_s is relative thickness of sand layer. C: Log (equivalent permeability ratio) vs. log (F_t) for DBF model (A, in black) and FWF model (B, in gray). Dashed lines are vertical equivalent permeability ratios; solid lines are horizontal ratios. Different T_s values are indicated on DBF model curves; note that vertical curves overlap. Error bars indicate range between maximum and minimum Cardwell-Parsons bounds for case of horizontal flow for different T_s values. These bounds are smaller than curve thickness for vertical-flow case.

ements or the above results: (1) In laboratory tests, permeability in an FWF damage zone remains higher than in the protolith and core as effective stress is increased (Evans et al., 1997). In addition, in situ fractures critically oriented for slip (i.e., those with high resolved shear stresses, the potentially active fractures) are highly permeable conduits at depths as great as 3.5 km (Barton et al., 1995). Thus, a large displacement normal FWF in a stress field favoring normal slip would likely be a vertical-flow conduit, owing to interconnected arrays of subvertical shear fractures in the damage zone. (2) Permeability of both undeformed sediments and deformed fine-grained sands and muds decreases significantly with increasing effective stress. The decrease is generally greater in finer-grained sediments (Brown et al., 1994; Haneberg et al., 1998). Because the clay core dominates the system, this last point suggests that increasing effective stress should further decrease the equivalent permeability ratio for a poorly lithified DBF.

An intermediate case between these two end members is that of a moderate- to large-displacement DBF in lithified, high-porosity sandstone. Deformation bands have significantly reduced permeability compared to their host rocks (e.g., Gibson, 1998), but the discrete slip surfaces act as open shear fractures, lending DBFs in lithified, high-porosity sandstones low fault-normal and potentially very high fault-parallel permeability (Antonellini and Aydin, 1995).

CONCLUSIONS

The internal architecture and lack of macroscopic fractures characteristic of large-displacement faults in poorly lithified sediments are easily identified in the field. The resulting bulk hydrologic properties significantly impede horizontal subsurface fluid flow at a regional scale and do not greatly enhance vertical flow, a condition much different from the conventionally accepted model of fault properties. These faults have significant potential to compartmentalize both aquifers and hydrocarbon reservoirs resulting in, for example, greater drawdown in production wells. Their low horizontal equivalent permeability suggests representation with a finer flow-model grid than would be necessary for faults with fractures. If faulting continues following lithification, prelithification structures may be preserved and/or overprinted with fractures. This may result in a fault with properties intermediate between the types discussed here. Depending on consolidation history, this transition may also be expected with increasing depth along a given fault.

ACKNOWLEDGMENTS

Support was provided by the National Science Foundation (grant EAR-9706482) and the New Mexico Geological Society. We thank Matt Davis and Christine Bowman for use of their permeameter, Andy Dunn for performing some of the consolidation tests, John Sigda for useful discussions, and Jim Evans and Darrel Cowan for their valuable reviews.

REFERENCES CITED

Antonellini, M., and Aydin, A., 1995, Effect of faulting on fluid flow in porous sandstones: Geometry and spatial distribution: American Association of Petroleum Geologists Bulletin, v. 79, p. 642–671.

Aydin, A., and Johnson, A.M., 1978, Small faults formed as deformation bands in sandstones: PAGEOPH, v. 116, p. 913–930.

Barton, C.A., Zoback, M.D., and Moos, D., 1995, Fluid flow along potentially active faults in crystalline rock: Geology, v. 23, p. 683–686.

Bredehoeft, J.D., Belitz, K., and Sharp-Hansen, S., 1992, The hydrodynamics of the Bighorn Basin: A study of the role of faults: American Association of Petroleum Geologists Bulletin, v. 76, p. 530–546.

Brown, K.M., Bekins, B., Clennell, B., Dewhurst, D., and Westbrook, G., 1994, Heterogeneous hydrofracture development and accretionary fault dynamics: Geology, v. 22, p. 259–262.

Caine, J.S., and Forster, C.B., 1999, Fault zone architecture and fluid flow: Insights from field data and numerical modeling, *in* Haneberg, W.C., et al., eds., Faults and subsurface fluid flow in the shallow crust: American Geophysical Union Geophysical Monograph 113, p. 101–127.

Caine, J.S., Evans, J.P., and Forster, C.B., 1996, Fault zone architecture and permeability structure: Geology, v. 24, p. 1025–1028.

Chester, F.M., Evans, J.P., and Biegel, R.L., 1993, Internal structure and weakening mechanisms of the San Andreas Fault: Journal of Geophysical Research, v. 98, p. 771–786.

Das, B.M., 1983, Advanced soil mechanics: Washington, D.C., Hemisphere Publishing, 511 p.

Evans, J.P., Forster, C.B., and Goddard, J.V., 1997, Permeability of fault related rocks, and implications for hydraulic structure of fault zones: Journal of Structural Geology, v. 19, p. 1393–1404.

Gibson, R.G., 1998, Physical character and fluid-flow properties of sandstone-derived fault zones, *in* Coward, M.P., et al., eds., Structural geology in reservoir characterization: Geological Society [London] Special Publication 127, p. 83–97.

Goodwin, L.B., Mozley, P.S., Moore, J.C., and Haneberg, W.C., 1999, Introduction, *in* Haneberg, W.C., et al., eds., Faults and subsurface fluid flow in the shallow crust: American Geophysical Union Monograph 113, p. 1–5.

Haneberg, W.C., 1995, Steady-state groundwater flow across idealized faults: Water Resources Research, v. 31, p. 1815–1820.

Haneberg, W.C., Gomez, P., Gibson, A., and Allred, B., 1998, Preliminary measurements of stress-dependent hydraulic conductivity of Santa Fe Group aquifer system sediments from the 98th St. core hole, Albuquerque, New Mexico: New Mexico Geology, v. 20, p. 14–20.

Hawley, J.W., 1996, Hydrogeologic framework of potential recharge areas in the Albuquerque basin, central New Mexico: New Mexico Bureau of Mines and Mineral Resources Open-File Report 402 D, chapter 1, 68 p.

Hawley, J.W., Haase, C.S., and Lozinsky, R.P., 1995, An underground view of the Albuquerque basin, *in* Proceedings, Annual Water Conference, 39th: New Mexico Water Resources Research Institute Report 290, p. 37–55.

Heynekamp, M.R., Goodwin, L.B., Mozley, P.S., and Haneberg, W.C., 1999, Controls on fault-zone architecture in poorly lithified sediments, Rio Grande rift, New Mexico: Implications for fault-zone permeability and fluid flow, *in* Haneberg, W.C., et al., eds., Faults and subsurface fluid flow in the shallow crust: American Geophysical Union Monograph 113, p. 27–49.

Knipe, R.J., 1993, The influence of fault zone processes and diagenesis on fluid flow, *in* Horbury, A.D., and Robinson, A.G., eds., Diagenesis and basin development: American Association of Petroleum Geologists Studies in Geology, no. 36, p. 135–151.

Mifflin, M.D., 1988, Region 5, Great Basin, *in* Back, W., et al., eds., Hydrogeology: Boulder, Colorado, Geological Society of America, Geology of North America, v. O-2, p. 69–78.

Morrow, C.A., Shi, L.Q., and Byerlee, J.D., 1981, Permeability and strength of San Andreas fault gouge under high pressure: Geophysical Research Letters, v. 8, p. 325–328.

Morrow, C.A., Shi, L.Q., and Byerlee, J.D., 1984, Permeability of fault gouge under confining pressure and shear stress: Journal of Geophysical Research, v. 89, p. 3193–3200.

Mozley, P.S., and Goodwin, L.B., 1995, Patterns of cementation along a Cenozoic normal fault: A record of paleoflow orientations: Geology, v. 23, p. 539–542.

Renard, P., and de Marsily, G., 1997, Calculating equivalent permeability: A review: Advances in Water Resources, v. 20, p. 253–278.

Sigda, J.M., Goodwin, L.B., Mozley, P.S., and Wilson, J.L., 1999, Permeability alteration in small-displacement faults in poorly lithified sediments: Rio Grande rift, central New Mexico, *in* Haneberg, W.C., et al., eds., Faults and subsurface fluid flow in the shallow crust: American Geophysical Union Monograph 113, p. 51–68.

Smith, D.A., 1980, Sealing and non-sealing faults in the Louisiana Gulf Coast salt basin: American Association of Petroleum Geologists Bulletin, v. 64, p. 145–172.

Thorn, C.R., McAda, D.P., and Kernodle, J.M., 1993, Geohydrologic framework and hydrologic conditions in the Albuquerque basin, central New Mexico: U.S. Geological Survey Water Resources Investigations Report 93-4149, 106 p.

Underhill, J.R., and Woodcock, N.H., 1987, Faulting mechanisms in high-porosity sandstones: New Red Sandstone, Arran, Scotland, *in* Jones, M.E., and Preston, R.M.F., eds., Deformation of sediments and sedimentary rocks: Geological Society [London] Special Publication 29, p. 91–105.

Yielding, G., Freeman, B., and Needham, D.T., 1997, Quantitative fault seal prediction: American Association of Petroleum Geologists Bulletin, v. 81, p. 897–917.

Manuscript received June 21, 2000
Revised manuscript received October 6, 2000
Manuscript accepted October 6, 2000

Printed in USA